

# Dynamic Multi-Channel TMS With Reconfigurable Coil

Ruoli Jiang, Ben H. Jansen, *Senior Member, IEEE*, Bhavin R. Sheth, and Ji Chen, *Senior Member, IEEE*

**Abstract**—Investigations of the causal involvement of particular brain areas and interconnections in behavior require an external stimulation system with reasonable spatio-temporal resolution. Current transcranial magnetic stimulation (TMS) technology is limited to stimulating a single brain area once in a given trial. Here, we present a feasibility study for a novel TMS system based on multi-channel reconfigurable coils. With this hardware, researchers will be able to stimulate multiple brain sites in any temporal order in a trial. The system employs a wire-mesh coil, constructed using  $x$ - and  $y$ -directional wires. By varying the current direction and/or strength on each wire, we can configure the proposed mesh-wire coil into a standard loop coil and figure-eight coil of varying size. This provides maximum flexibility to the experimenter in that the location and extent of stimulation on the brain surface can be modified depending on experimental requirement. Moreover, one can dynamically and automatically modify the site(s) of stimulation several times within the span of seconds. By pre-storing various sequences of excitation patterns inside a control unit, one can explore the effect of dynamic TMS on behavior, in associative learning, and as rehabilitative therapy. Here, we present a computer simulation and bench experiments that show the feasibility of the dynamically-reconfigurable coil.

**Index Terms**—Electromagnetic modeling, magnetic stimulation, reconfigurable coil.

## I. INTRODUCTION

**M**OST behaviors arise from complex interactions between distant anatomical areas. These areas receive neural information asynchronously in time. To investigate behavior while still maintaining the timing of information that occurs during real sensory stimulation, an external stimulation system with reasonable spatio-temporal resolution is needed. Transcranial magnetic stimulation (TMS) is such a technology that provides an external stimulus at a single brain site with high spatial resolution. Transcranial magnetic stimulation uses the principle of inductance to couple electrical energy across the scalp and skull without the pain of direct percutaneous electrical stimulation. That is to say, a time-varying magnetic field can generate induced currents within a conducting medium, such as human nervous tissue or muscle. TMS involves placing a small coil or coils of wire on the scalp and

passing a powerful and rapidly changing current pulse through it [1]. This produces a magnetic field, which passes relatively unimpeded through skin, scalp, and skull, and is tolerated well by most humans. This magnetic field induces a weak electrical current in the brain. The strength of the induced current is a function of the rate of change of the magnetic field as well as of the conductivity of the medium. The induced current may depolarize or hyperpolarize the underlying population of neurons in the cortex, which are known to fire spikes or action potentials at rates approaching one every 10 ms. If the induced current is parallel to the nerve fiber, it can lead to a greater change in the membrane potential which may excite the nerve cell [2]. Accurate, temporally discrete delivery of a time-varying magnetic field within a circumscribed brain region is critical. At present, the most efficient way to deliver a time-varying magnetic field within human subjects is through magnetic coils. Most current technologies are focused on using either a single loop coil or figure-eight coil, thus limiting TMS technology to a single brain region and a single time instant. Although multi-channel TMS designs have been proposed [3], such systems lack flexibility in their designs. Many individual coils are used as elements to achieve a “multi-channel effect” [4]. Attempts have been made towards developing a coil-positioning and holding system that can fix the relative position between a single coil and skull [5], however there is no system, to our knowledge, that can fix the position of multiple coils on the skull. As a result, multi-channel TMS is not currently available. We are developing a novel TMS system based on computer-controlled multi-channel reconfigurable coils that can stimulate multiple sites, separated by no more than a few centimeters, simultaneously and/or in rapid succession (at a time-scale of 100 ms or better). With this hardware, researchers will be able to reproducibly stimulate multiple sites on the patient’s brain with a spatio-temporal pattern preprogrammed by the experimenter. Creating a multi channel TMS coil system that allows for simultaneous or paired (triple, quadruple, etc.) stimulation on multiple locations without moving the coil would facilitate how studies are done including improvement in stimulation blinding, reducing experimental time by avoiding coil movement to target multiple sites, and improving “virtual lesion” study designs by disrupting multiple nodes of a cortical network. It would open the opportunity to do newer studies such as modulation of cortical network activity by manipulating in a Hebbian-like manner how distant cortical sites communicate. Also, the device may prove to be more effective in the treatment of a variety of psychiatric and behavioral disorders than present TMS technology.

In this paper, we demonstrate the theoretical feasibility of the device on the basis of computer simulations and bench experiments.

Manuscript received October 14, 2011; revised February 23, 2012, June 12, 2012, July 31, 2012; accepted October 07, 2012. Date of publication November 16, 2012; date of current version May 04, 2013. This work was supported by the National Institutes of Health (NIH) under Grant R21-MH07904.

The authors are with the Department of Electrical and Computer Engineering, University of Houston, Houston, TX 77204 USA (e-mail: bjansen@uh.edu).

Color versions of one or more of the figures in this paper are available online at <http://ieeexplore.ieee.org>.

Digital Object Identifier 10.1109/TNSRE.2012.2226914

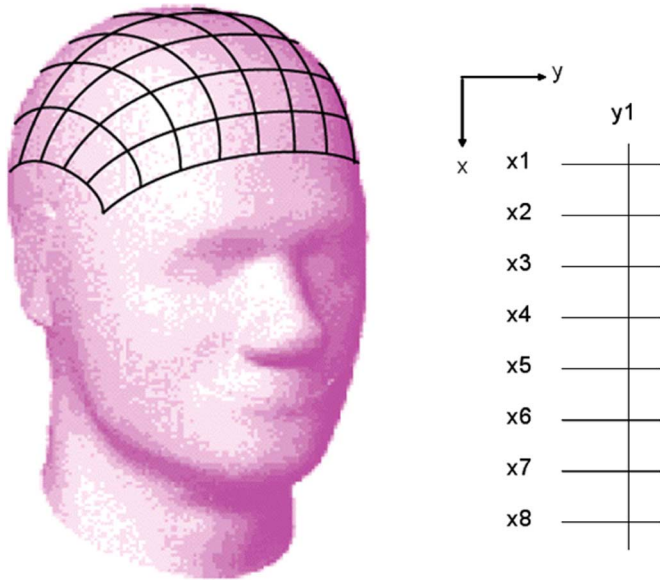


Fig. 1. Illustration of a wire-mesh coil. On the left it is shown how the coil conforms to the head. A flattened, and expanded 2-D version of the coil is shown on the right. The actual spacing between adjacent wires is not drawn to scale.

## II. DYNAMIC MULTI-CHANNEL COIL

We are developing a wire-mesh coil, as illustrated in Fig. 1. It is constructed using  $x$ -directional and  $y$ -directional wires, laid relatively close to each other but otherwise electrically insulated. The  $x$  and  $y$  directions correspond to the anterior–posterior and mediolateral axes, respectively. By varying the current direction/strength on each wire, we can configure this mesh-wire coil into a standard loop coil and figure-eight coil of varying size. This provides maximum flexibility in that the location and extent of stimulation on the brain surface can be modified depending on experimental requirements. The two top panels in Fig. 2 illustrate two configured loop coils of different sizes. By selecting current strength  $y_2 = I$ ,  $y_3 = -I$ ,  $x_2 = I$ ,  $x_3 = -I$ , and setting the current strength to zero on the other wires, we can configure a small loop in the coil. If, on the other hand, if we select  $y_2 = I$ ,  $y_5 = -I$ ,  $x_2 = -I$ ,  $x_5 = I$ , and zero current flow on the other wires, we will configure a larger loop than before using the same wire-mesh coil. The two bottom panels of Fig. 2 illustrate how figure-eight coils of different sizes can be configured using the same wire-mesh design.

The proposed wire-mesh coil has the potential to dynamically alter the pattern of TMS across the expanse of the cortical surface within milliseconds. While we aim for no more than a 100 ms inter-stimulus interval (ISI), the actual ISI could be shorter, depending on the number and recharge time of the power units that provide the current pulses. Fig. 3 illustrates the technique of dynamic TMS by simply switching on/off current in different wires to achieve various figure-eight coil configurations at different time instances. By pre-storing various on/off current sequences inside a control unit, we can explore the effect of dynamic TMS on behavior, learning, and therapy.

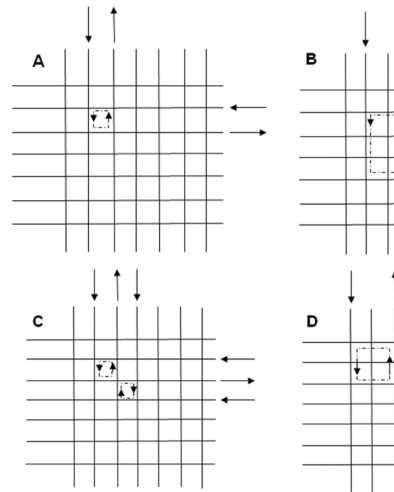


Fig. 2. Configured loop coils and figure-eight coils of differing size. A: Small loop coil is configured by setting two pairs of adjacent wires running currents in opposite direction. B: Large loop coil is configured by setting two-pairs of non-adjacent wires running currents in opposite direction. C: Small figure-eight coil is configured by setting three adjacent wires running currents in positive–negative–positive directions. D: Large figure-eight coil is configured by setting three nonadjacent wires running currents in positive–negative–positive directions.

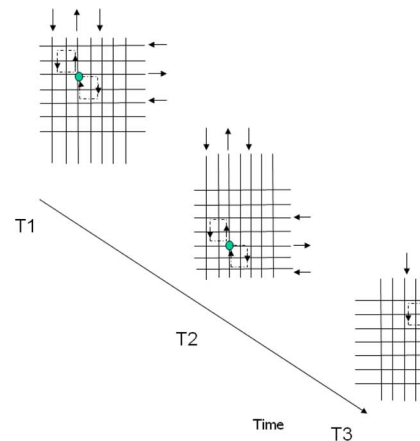


Fig. 3. An illustration of the proposed dynamic procedure using the proposed reconfigurable coil. At time  $t = T1$ , a figure-eight is configured at the top left corner of coil. At time  $t = T2$ , a figure-eight coil is configured at the bottom-left corner of the coil. At time  $t = T3$ , a figure-eight coil is configured at the midright section of the coil. The time instances  $T1$ ,  $T2$ , and  $T3$  are on the order of tens of milliseconds.

## III. RESULTS

Results obtained through computer simulations and bench measurements supporting the feasibility of the proposed dynamic TMS device are presented here. In all these experiments a planar (not head-conformal) version of the wire mesh coil was used.

### A. Simulation Studies

Preliminary simulations have been done to explore the feasibility of the wire-mesh coil. A wire-mesh coil with a 5 cm spacing between adjacent wires was placed 0.5 cm above a phantom of 30 cm  $\times$  30 cm  $\times$  30 cm. The conductivity of the phantom was set at 0.1 S/m to approximate the brain's conductivity [6], and a unit current of 60 Hz was applied to the coil. Although TMS is working at much higher frequencies

(3.5–10 kHz), under the quasi-static assumption, the results will still be approximately the same. The induced currents were sampled at a plane 2.5 cm below the coil. This corresponds roughly to the location of the cortex below the skull, although in real life some cortical areas will be positioned deeper due to the convoluted shape of the cortex. Simulation was performed using a rigorous 3-D impedance method based on a generalized version presented in [7]. In the impedance method, the phantom model is first discretized into small cubes (after some experimentation, we obtained convergence for cubes with dimension 5 mm × 5 mm × 5 mm). Each cube is modeled by an elementary impedance network and the entire head model is represented by an end-to-end cubic tessellation. In [7], each cubic element was modeled as a resistor, accounting for the conductive loss of the tissue. This is appropriate at low frequencies, however, as the frequency increases, the dielectric constant introduces an additional capacitive effect via impedance  $Z = 1/j\omega C$ . Therefore, we modeled the electrical behavior of each cubic element by a capacitor and resistor in parallel. At low frequencies, the capacitors act like open circuits, leading to the purely resistive network of [7]. The values of the capacitor and the resistor are determined by the electrical properties of the cubic element. For example, the resistor value is given by  $R = dz/(dx \cdot dy \cdot \sigma)$ , where  $dx$ ,  $dy$ , and  $dz$  represent the dimensions of the cubic element, and  $\sigma$  is the conductivity in the cubic element, which is determined here by the biological tissue residing inside the element [6]. Similarly,  $C = \epsilon \cdot dx \cdot dy/dz$ , with  $\epsilon$  the permittivity of the tissue inside the cubic element. Connecting together the equivalent circuit of all the cubic elements leads to the formation of a complex impedance network [8]. The simulation starts with obtaining the external magnetic field generated by the TMS coil and then evaluating the induced current within the biological tissue. Using this impedance method, the induced current density ( $A/m^2$ ) generated by the small loop coil [Fig. 2(A)], and the small figure-eight coil [Fig. 2(C)] were computed and they are shown in Fig. 4. The top two plots show the induced current densities generated by the two configured coils in a plane located 2.5 cm below the coil. The leftmost bottom panel of Fig. 4 shows the induced current densities along the  $x$  direction of the small coil, while the rightmost bottom panel shows the induced current density along the diagonal direction when the figure-eight coil was configured. These results show clearly that the reconfigurable coil can generate various induced-current patterns inside the phantom and achieve adequate spatial resolution on the order of 5 cm, which is comparable to current figure-eight coil resolution [9]. If wires are placed closer together, higher resolution can be achieved. In the simulation, all currents were normalized to 1 A to prove the feasibility of the coil's reconfigurability. The actual current strength will be large enough to generate a magnetic field strength of around 1.5–2T near the surface of the coil and about 0.4T three cm under the coil [9].

### B. Bench Experiments

In addition to numerical verifications, experimental investigations have been performed to further validate the proposed approach using the setup shown in Fig. 5. Grooves 3 mm wide were cut in a 35 cm × 35 cm plywood board. Eight of

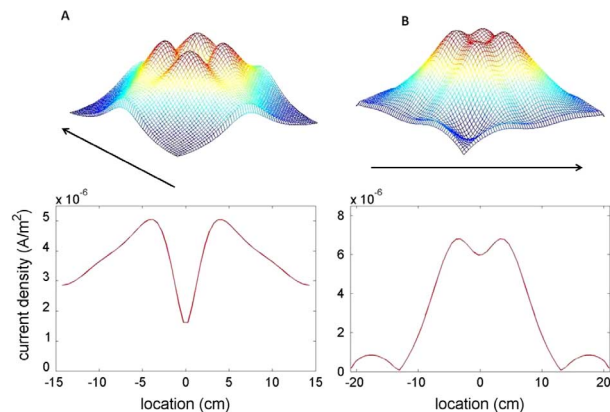


Fig. 4. Induced current densities generated by reconfigured small loop coil (A) and small figure-eight coil (B). The two top figures show the induced current density in the plane that is 2.5 cm below the coil configuration. The bottom panels show the induced current densities along the directions indicated by the arrows below the top panels (i.e., the  $x$  direction of the configured small loop coil, and the diagonal direction of configured figure-eight coil).

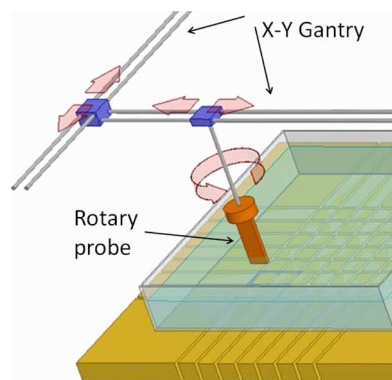


Fig. 5. The setup for the bench experiments. Shown are the grooved board containing the figure-eight wire mesh coil, the saline container, and rotary probe suspended from a computer-controlled gantry.

the grooves ran parallel to each other with a 15 mm spacing between grooves, and eight similarly-shaped grooves were cut perpendicular to the first eight. Multi-strand copper wire was placed in the grooves following the pattern shown in Fig. 2(C) to form a small figure-eight coil. A plastic container filled with a saturated solution of pure salt (NaCl) in water was placed on top of the board to simulate the environment inside the skull. The figure-eight coil was connected to a Magstim Rapid stimulator (Magstim, Wales, U.K.) which provided the current pulses. A rotary loop probe was suspended from a computer-controlled gantry, which allowed for accurate placement of the probe in the  $(x, y)$  plane. The voltage generated in the loop probe is proportional to the change in the magnetic field ( $dB/dt$ ) generated by the coil. For each position in the  $(x, y)$  plane, three measurements of the maximum voltage generated in the probe were taken, and averaged.

Fig. 6 shows the voltage distribution measured 1 cm above the plane where the coil resides. Two regions with relatively large voltages, and thus strongly changing magnetic fields, enclosed by circles in Fig. 6, can be observed.

Presently, due to hardware limitations, we cannot perform direct induced current measurement within a phantom. However,

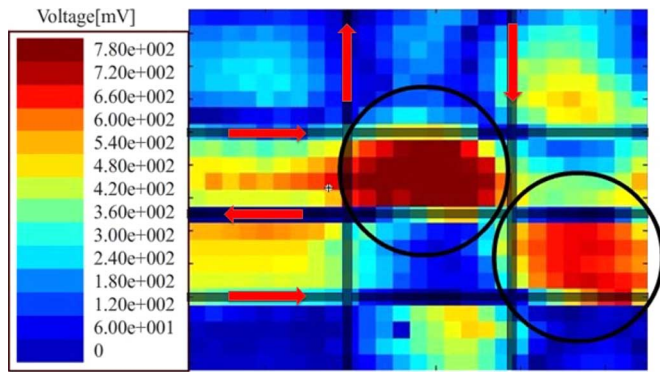


Fig. 6. Maximum voltage, proportional to  $dB/dt$  measured 1 cm above plane of wire-mesh coil. Straight lines show the location of the wires that make up the mesh coil, and arrows show the direction of the current through the wires. The circles denote the areas with high magnetic field.

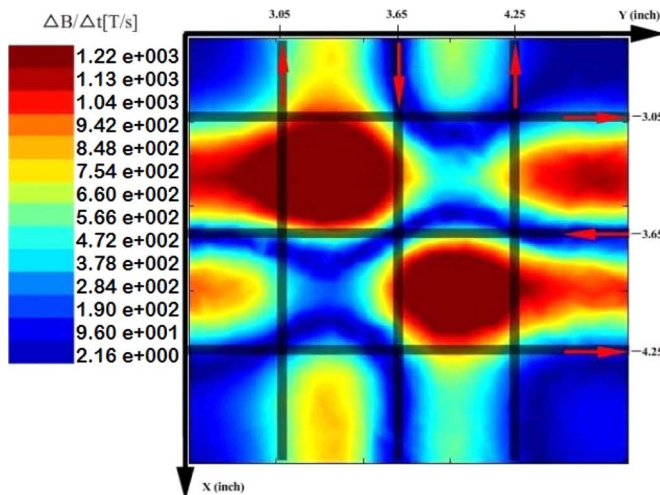


Fig. 7. Time derivative of the magnetic field ( $dB/dt$ ) as obtained through simulation with Ansoft Maxwell. Arrows indicate direction of the current through the wires.

the Ansoft Maxwell software package (ANSYS, Inc., Canonsburg, PA, USA) was used to simulate the (time derivative of the) magnetic field distribution on the same plane as that of the measurement (the simulated  $dB/dt$  is shown in Fig. 7) and the induced current inside the saline solution (shown in Fig. 8) in response to a 6000 A current pulse with a 1 ms duration. The current pulse was designed to match a typical pulse used in TMS system, linearly increasing from 0 to 6000 A in 0.1 ms, staying at 6000 A between 0.1 and 0.2 ms and linearly decreasing to 0 A increased over the 0.2 to 1.0 ms interval. The conductivity of the saline solution was set at 4.8 S/m and the relative permittivity to 81. Ansoft Maxwell is a program that implements the finite elements method, and we used 50 000 tetrahedron-shaped elements, distributed over a volume of  $10.3 \times 10.3 \times 3$  in, covering the saltwater area, with 20 000 elements contained in a cube of  $2.3 \times 2.3 \times 2$  in positioned directly over the coil. Fig. 7 shows a strong correlation between the measurement results presented in Fig. 6. Furthermore, the simulations presented in Fig. 8 show that a concentrated electric current is indeed induced under the coil further validating the feasibility of this novel coil.

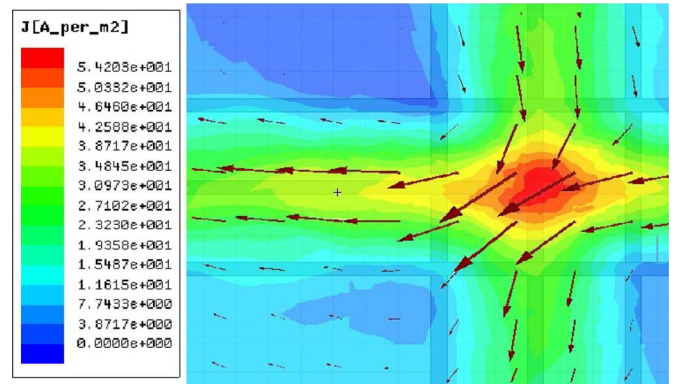


Fig. 8. Induced current as obtained through simulation with Ansoft Maxwell. Arrows indicate size and direction of the current. The direction of the current through the wires is the same, as in Fig. 7.

It is also clear that the results of the bench experiments deviate from the simulations to some degree. Specifically, the amplitudes of the induced currents/magnetic fields are not identical in the two leaves that comprise the figure-eight coil. This is attributable to several factors. First, the wire-mesh coil was hardwired, passing a single wire through the groves and looping around the board where needed. Because the wire-mesh coil is not centered in the grooved board, the wires looping around the board affect the leaves of the coil electromagnetically in a non-balanced manner. Also, a  $17 \mu\text{H}$  inductance to provide proper loading of the Magstim stimulator sits under the board and is connected in series with the power supply and mesh coil. While this coil is shielded with a grounded copper plate, the shielding does not provide a perfect Faraday cage and the loading coil's electromagnetic field will have additional distorting effects on the induced currents/magnetic fields. One should also note that there are no open wires in this setup.

#### IV. CONCLUSION

The wire-mesh reconfigurable coil proposed here uses an easy to fabricate 2-D ( $x, y$ ) head-conformal structure and has the following characteristics.

- 1) *Easy fabrication and design.* Our design needs fewer wires in the mediolateral ( $x$ ) and anterior–posterior ( $y$ ) directions (16 in our design as compared to 162 in [3]). Optimal design parameters for wire diameter and inter-wire spacing, which will determine the current-carrying capability and spatial resolution of the wire mesh, can be easily obtained from current knowledge.
- 2) *Low cost.* If there are  $N$  wires each in the  $x$  and  $y$  directions, at most  $2N$  current control units (switches) are required compared to the  $N^2$  control units in [3]. Also, we will need at most as many current units as sites to be stimulated provided that the recharge time of the units is less than the interval between successive stimulations. Current single channel commercially-available repetitive TMS systems can stimulate up to 30 times/s (33 ms time resolution) with little fall-off in power, thus facilitating the intended 100 ms ISI.

- 3) *Easy synchronization.* In a multi-channel coil design, it is difficult to synchronize the individual elements so that they will launch the current at exactly the same time instant. For the proposed wire-mesh coil, this difficulty is greatly reduced since only  $2N$  control units need to be synchronized compared to the  $N^2$  units in [3].
- 4) *Coil rigidity.* A problem with multi-channel coils is that the position of each element needs to be individually controlled, which may lead to relative movement of the different coils. Relative movement among coil elements is likely to defocus the delivered magnetic field under the coil and reduce spatial reliability from trial to trial. Our reconfigurable coil can be constructed using a single rigid piece, eliminating the relative movement among individual wires.

The wire mesh coil as proposed here has its limitations as well. For example, the current induced by a figure-eight coil will be perpendicular to the line connecting the centers of the two leaves of the coil. In case of a conventional, hand-held coil, the induced current's direction can be altered by rotating the coil. In contrast to the conventional figure-eight coil and the multi-channel device presented in [10], our proposed coil can produce only four current directions ( $45^\circ$ ,  $135^\circ$ ,  $225^\circ$ , and  $315^\circ$ ) by reversing the current and/or moving the two leaves of the figure eight from the second and fourth quadrant to the first and third, respectively. Should none of these (discrete) current directions be adequate, we may have to resort to a loop coil. Alternatively, a multi-layered coil could be designed, with additional layers oriented at an angle to the underlying layer(s). For example, in a dual-layer coil (formed with one layer stacked over another one), with the second layer oriented  $45^\circ$  to the first, four additional current directions ( $0^\circ$ ,  $90^\circ$ ,  $180^\circ$ , and  $270^\circ$ ) can be obtained.

The bench experiments and simulations show that we can generate focused magnetic fields and induced currents, but there are also significant fields and currents outside the intended stimulation area arising from the wires feeding the dynamically-configured loop or figure-eight coil. The stray fields will negatively affect the focalization of the delivery of the induced current. Also, although these fields are smaller than under the configured coil, it is unclear what their consequences in terms of hyperpolarization and depolarization of nerve tissue will be. However, it may be possible to reduce these peripheral fields and currents using a multi-layer design of the wire mesh coil, with a second layer configured to selectively enhance or counteract currents in the first layer.

There is still a lot of work that needs to be done before the dynamically-reconfigurable coil is ready for use. Several major issues remain. The first issue is the design of the solid-state switches needed to allow or restrict the flow of the large current (well above 1000 A) to the wires that make-up the wire-mesh coil. Integrated gate-commutated thyristors (IGCTs) can be used, providing rapid ( $12 \mu\text{s}$ ) turn-off behavior, but they are rather expensive and we are searching for a more cost-effective solution.

Another issue is that the coil's inductance will vary as a function of the wire mesh configuration. Consequently, the stimulus waveform will change as the coil's configuration changes. In

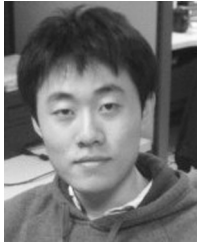
fact, the inductance is roughly proportional to the diameter of the coil (assuming no changes in number of loops, wire diameter, etc.), so these changes could be significant. Depending on the severity of the problem, we may have to employ a variety of stimulus generators to maintain waveform stability. However, if only the location of the coil within the mesh changes, and not its size or configuration (i.e., loop or figure eight), there should be no change in inductance.

Last, but not least, is the mutual coupling among coils when large currents are switched rapidly on or off. When two coils are close to each other, the current variation in one coil typically leads to a secondary current in the other coil, which will compromise the spatial resolution of the stimulation. The capacitive coupling can be minimized by grounding the active wires. The inductive coupling can be minimized by leaving nonactive wires open, i.e., terminating them with a very large resistance ( $>10 \text{ k}\Omega$ ). The resistance in regular wires is less than  $1 \Omega$ ; therefore, with such a high ratio of resistance (10 000:1), the induced current on the unused wires will be much lower than in the active coil, and the mutual coupling will be negligible.

The wire mesh design proposed here makes it also possible to avoid using coils at all; as pointed out to us during the review phase of this manuscript, two orthogonal current-carrying wires that cross each other would generate an induced current with magnitude of  $\sqrt{2}$  as compared to a single wire. The resulting induced current would be more focused than one generated by a figure-eight or loop coil.

## REFERENCES

- [1] M. Hallett, "Transcranial magnetic stimulation and the human brain," *Nature*, vol. 40, pp. 147–150, Jul. 13, 2000.
- [2] S. Ueno, "Localized magnetic stimulation and nerve excitation models," *Adv. Occupat. Med. Rehabil.*, vol. 2, no. 2, pp. 25–39, May–Aug. 1996.
- [3] J. Ruohonen and R. Ilmoniemi, "Multichannel magnetic stimulation: Improved stimulus targeting," *Adv. Occupat. Med. Rehabil.*, vol. 2, no. 2, pp. 55–64, May–Aug. 1996.
- [4] M. Lu, S. Ueno, T. Thorlin, and M. Persson, "Calculating the current density and electric field in human head by multichannel transcranial magnetic stimulation," *IEEE Trans. Magnetics*, vol. 45, no. 3, pp. 1662–1665, Mar. 2009.
- [5] D. A. Bohning, S. Denslow, P. A. Bohning, J. A. Walker, and M. S. George, "A TMS coil positioning/holding system for MR image-guided TMS interleaved with fMRI," *Clin. Neurophysiol.*, vol. 114, pp. 2201–2219, 2003.
- [6] S. Gabriel, R. W. Lau, and C. Gabriel, "The dielectric properties of biological materials, III. Parametric models for the dielectric spectrum of tissues," *Phys. Med. Biol.*, vol. 41, pp. 2271–2293, 1996.
- [7] M. Nadeem, M. Persson, and O. P. Gandhi, "Computation of electric and magnetic stimulation in human head using the 3D impedance method," *IEEE Trans. Biomed. Eng.*, vol. 50, no. 7, pp. 900–907, Jul. 2003.
- [8] N. Orcutt and O. P. Gandhi, "A 3-D impedance method to calculate power deposition in biological bodies subject to time varying magnetic fields," *IEEE Trans. Biomed. Eng.*, vol. 35, no. 8, pp. 577–583, Aug. 1988.
- [9] J. Ruohonen, M. Ollikainen, V. Nikouline, J. Virtanen, and R. J. Ilmoniemi, "Coil design for real and sham transcranial magnetic stimulation," *IEEE Trans. Biomed. Eng.*, vol. 47, no. 2, pp. 145–148, Feb. 2000.
- [10] J. Ruohonen and R. J. Ilmoniemi, "Focusing and targeting of magnetic brain stimulation using multiple coils," *Med. Biol. Eng. Comput.*, vol. 36, pp. 297–301, 1998.



**Ruoli Jiang** received the B.S. degree in electrical and information engineering from the Huazhong University of Science and Technology, Wuhan, China, in 2010. He is currently working toward the Ph.D. degree in electrical engineering at the University of Houston, Houston, TX, USA.

His research is concerned with the development of electromagnetic devices for brain stimulation and cell sorting.



**Bhavin R. Sheth** received the B.S. and M.S. degrees in computer science and the M.S. degree in electrical engineering from the University of Southern California, Los Angeles, CA, USA, and the Ph.D. degree in cognitive neuroscience from the Massachusetts Institute of Technology, Cambridge, MA, USA.

He is an Associate Professor in the Electrical and Computer Engineering Department, University of Houston, Houston, TX, USA. His major area of research is concerned with human sensory information processing.



**Ben H. Jansen** (S'74–M'76–SM'90) received the B.S. and M.S. degrees in electrical engineering from Twente University, Enschede, The Netherlands, and the Ph.D. degree in medical informatics from the Medical School, Free University, Amsterdam, The Netherlands.

He is a Professor in the Electrical and Computer Engineering, and the Biomedical Engineering Departments, University of Houston, Houston, TX, USA. His major area of research is concerned with the spontaneous and evoked

activity generated by the (human) brain.



**Ji Chen** (S'87–M'90–SM'07) received the B.S. degree from Huazhong University of Science and Technology, Wuhan, China, the M.S. degree from McMaster University, Hamilton, ON, Canada, in 1994, and the Ph.D. degree from the University of Illinois, Urbana-Champaign, IL, USA, in 1998, all in electrical engineering.

He is currently an Associate Professor with the Department of Electrical and Computer Engineering, University of Houston, Houston, TX, USA. His research interests include computational

electromagnetic, modeling and design of biomedical instruments, stochastic analysis of periodic structure and nonperiodic structures, and characterization of composite materials. Prior to joining the University of Houston, from 1998 to 2001, he was a Staff Engineer with Motorola Personal Communication Research Laboratories, Chicago, IL, USA.

Dr. Chen has received an outstanding teaching award and an outstanding junior faculty research award from Cullen College of Engineering at the University of Houston. He is also the recipient of ORISE fellowship in 2007. His research group also received the best student paper award at the IEEE EMC Symposium 2005 and the best paper award from the IEEE APMC conference in 2008.